AD-A145 679 ONE-DIMENSIONAL TWO-PHASE CONSTANT LAG FLOW IN 1/1
COMBUSTION CHAMBER OF SOLI..(U) FOREIGN TECHNOLOGY DIV
WRIGHT-PATTERSON AFB OH C HSIEN'CH'I 15 AUG 84
UNCLASSIFIED FTD-ID(RS)T-0880-84 F/G 21/2 NL

END
DATE FILMED
10-84
DTIC

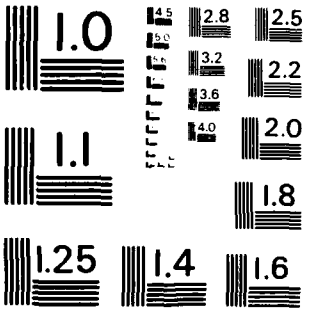

FTD-ID(RS)T-0880-84

FOREIGN TECHNOLOGY DIVISION

ONE-DIMENSIONAL TWO-PHASE CONSTANT LAG FLOW IN COMBUSTION CHAMBER OF SOLID PROPELLANT ROCKET MOTORS

by

Ch'ang Hsien-ch'i

EDITED TRANSLATION

FTD-ID(RS)T-0880-84 15 Aug 1984

MICROFICHE NR: FTD-84-C-000817L

ONE-DIMENSIONAL TWO-PHASE CONSTANT LAG FLOW IN COMBUSTION CHAMBER OF SOLID PROPELLANT ROCKET MOTORS

By: Ch'ang Hsien'ch'i

English pages: 21

Source: Yuhang Xuebao, Nr. 4, 1983, pp. 40-52

Country of origin: China
Translated by: SCITRAN
F33657-81-D-0263
Requester: FTD/TQTA

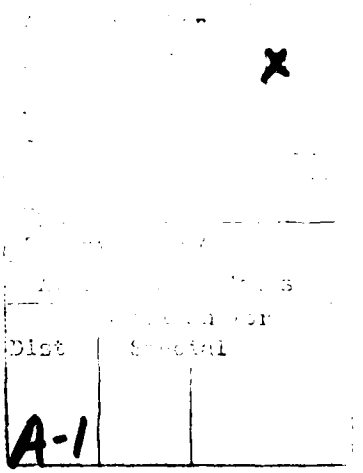

PREPARED BY:

TRANSLATION DIVISION
FOREIGN TECHNOLOGY DIVISION
WP-AFB, OHIO.

GRAPHICS DISCLAIMER

All figures, graphics, tables, equations, etc. merged into this translation were extracted from the best quality copy available.

ONE-DIMENSIONAL TWO-PHASE CONSTANT LAG FLOW IN COMBUSTION CHAMBER OF SOLID PROPELLANT ROCKET MOTORS /1*

Ch'ang Hsien-ch'i

Abstract

In this paper, one-dimensional two-phase constant lag flow in combustion chamber of solid propellant rocket motors is described. Introducing a specific heat ratio $\bar{K}$ and a gas constant $\bar{R}$ for constant lag flow, fundamental relationships analogous to those of pure gas flow are derived. The effect of particle velocity lags on pressure-time curves and flow field in chamber is analyzed.

Main Notations

A_b - Combustion area of grain
A_p - Cross-sectional area of passage
A_Q - Mechanical equivalent of heat
A_t - Area of nozzle throat
b - Coefficient of combustion rate
C^* - Characteristic velocity of propellant
C_1 - Particle specific heat
C_{Pg} - Constant-pressure specific heat of gas phase
C_{Vg} - Constant-volume specific heat of gas phase
g - Gravitational acceleration
h - Enthalpy per unit weight
H_s - Total enthalpy of 1 kg of products of combustion
J - Throat-passage ratio
k - Specific heat ratio of gas phase
K,L - Lag constants
K_1 - Surface-throat ratio
l - Length of grain

This paper was received on November 29, 1982.

*Figures in margin designate foreign pagination.

m_p - particle mass flow

$\dot{m}$ - Mass flow of mixture of two phases

$\dot{m}_g$ - Mass flow of gas phase

n - Index of pressure

P - Pressure

P_s - Total pressure

P_r - Prandtl's number

r - Combustion rate

r_p - Radius of particle

R_g - Gas constant of gas phase

S - Perimeter of passage

t - Time

T - Temperature

T_0 - Total temperature of gas phase at the head of the grain

v - Flow rate

W - Jet velocity

x - Axial coordinate

$\bar{x}$ - Relative axial coordinate $\bar{x}=\frac{x}{l}$

ρ - Density

ρ_r - Density of propellant

$\rho_{Al_2O_3}$ - Density of Al_2O_3

ε - Partial particle mass flow, $\varepsilon=\frac{\dot{m}_p}{\dot{m}}$

λ_g - Coefficient of thermal conduction of gas

μ_g - Coefficient of dynamic viscosity of gas

Subscripts /2

g - Gas phase

O - Cross-section of grain head

t - Cross-section of nozzle throat

P - Particle phase

L - Cross-section of tail end of grain

I. Foreword

Al_2O_3 particles are formed when composite solid propellants containing aluminum undergo combustion. Their fractional weight may reach 30-40%. Thus, there is a mixture of two phases (gas and particle) in the products of combustion that flow in the combustion chamber and the nozzle.

Most of the current studies on two-phase flows in solid propellant rocket engines focus on the nozzle. Kliegel studied one-dimensional two-phase constant lag nozzle flow, and obtained a solution similar to that for isentropic flow[2].

The two-phase flow in the combustion chamber is one which involves mass, and possesses some new characteristics in comparison with that in the nozzle. In this paper, we describe one-dimensional two-phase constant lag flow in the combustion chamber, and analyze the effect of particle velocity lags on the pressure-time curves and the flow field in the combustion chamber. This is helpful for accurately predicting the pressure-time curve, and provides more precise boundary conditions for computing two-phase nozzle flows.

II. Governing Equations

Assume that:[1],[2]

1. The flow is one-dimensional and pseudo-steady-state.

2. The friction and heat conduction between the flow and the passage walls are neglected.

3. The Al_2O_3 particles are uniform in size, and are in fluid state. The spatial volume occupied by these particles as well as the effect of their Brownian motion on pressure are neglected.

4. The gas phase is an ideal gas with frozen components. It has no viscosity except where it is in contact with the particles.

5. The force exerted by mass is neglected.

Accordingly, we have derived from Ref. [1] the governing equations for the two-phase mixture in the grain passage of constant cross-section:

Mass equation

$$\frac{dm}{dx}=\rho_T r S \tag{1}$$

Momentum equation

$$\frac{d}{dx}(\rho_g v_g^2+\rho_p v_p^2)=-\frac{dP}{dx} \tag{2}$$

Energy equation

$$\frac{d}{dx}\left[m_g\left(h_g+A_Q\frac{v_g^2}{2g}\right)+m_p\left(h_p+A_Q\frac{v_p^2}{2g}\right)\right]=\rho_T r S H_s \tag{3}$$

From $m=m_p+m_g$ and $\frac{m_p}{m}=e$, , taking Eq. (1) into consideration, we can write Eq. (3) as

$$\frac{d}{dx}\left\{\left[(1-e)\left(h_g+A_Q\frac{v_g^2}{2g}\right)+e\left(h_p+A_Q\frac{v_p^2}{2g}\right)-H_s\right]\cdot m\right\}=0 \tag{4}$$

Integrating Eqs. (2) and (4) (when x = 0, $v_g = v_p = 0$, /3 $\dot{m} = 0$), we obtain, respectively, the integral form of the momentum equation and the energy equation of the two phase mixture:

$$P_0-P=\rho_g v_g^2+\rho_p v_p^2 \tag{5}$$

$$(1-\varepsilon)\left(h_g+A_Q\frac{v_g^2}{2g}\right)+\varepsilon\left(h_p+A_Q\frac{v_p^2}{2g}\right)=H_s \tag{6}$$

III. Fundamental Relations of Constant Lag Flows

Define $$K\equiv\frac{v_p}{v_g}\qquad(0\leqslant K\leqslant 1) \tag{7}$$

$$L\equiv\frac{T_g-T_p}{T_*-T_g}\ (0\leqslant L\leqslant 1) \tag{8}$$

Then, particle velocity lag $$\equiv\frac{v_g-v_p}{v_g}=1-K \tag{9}$$

particle temperature lag $$\equiv\frac{T_p-T_g}{T_*-T_g}=1-L \tag{10}$$

The so-called constant lag flow refers to the two-phase flow in which K and L remain constant along the length of the passage.

1. Temperature Ratio $\frac{T_g}{T_*}$

When the temperature of the Al_2O_3 particles exceeds 2318°K, the specific heat of Al_2O_3 is a constant, and

$$h_p=h_{pm}+C_l(T_p-T_{pm})^{[1]}.$$

In the above relation, h_{Pm} is the enthalpy of liquid Al_2O_3 at the temperature T_{Pm} - 2318°K.

Denote the total enthalpy of 1 kg of the gas phase and that of 1 kg of the particle phase by h_{sg} and h_{sP}, respectively. Then the total enthalpy of 1 kg of the two-phase mixture is

$$H_s=(1-\varepsilon)h_{sg}+\varepsilon h_{sp}$$

From Assumption 2 above we know the H_S remains constant along the length of the passage. Let us, therefore, express H_S in terms of the parameters ($f_g = v_P = 0$, $T_g = T_p = T_O$) at the grain head. Thus,

$$H_s=(1-\varepsilon)C_{pg}T_0+\varepsilon[h_{pm}+C_l(T_0-T_{pm})]$$

Inserting the expressions for H_S and h_P above, as well as $h_g = C_{Pg}T_g$ into Eq. (6), and taking note of Eqs. (7) and (8), we obtain the energy equation for the constant lag two-phase mixture:

$$\bar{C}_pT_g+A_0\frac{v_2^2}{2g}=\bar{C}_pT_0 \tag{11}$$

In the above equation,

$$\bar{C}_p=\frac{(1-\varepsilon)C_{pg}+\varepsilon C_lL}{1-\varepsilon+\varepsilon K^2}=C_{pg}\cdot\frac{1+\frac{\varepsilon}{1-\varepsilon}\delta L}{1+\frac{\varepsilon}{1-\varepsilon}K^2} \tag{12}$$

$$\delta=\frac{C_l}{C_{pg}}$$

It can be seen from Eq. (11) that the form of the energy equation for constant lag two-phase mixture in the combustion chamber is the same as that for pure gas phase flow. We /4 refer to $\bar{C}_p$ as the constant-pressure specific heat of constant lag flow. Note, however, that this is not the constant-pressure specific heat of the two-phase mixture, but rather a symbol introduced so as to be able to write the equation in the form of that for pure gas phase. The total temperature T_O at the grain head is equal to the combustion temperature of the grain.

Similarly, the constant lag constant-volume specific heat

$$\bar{C}_v = \frac{(1-\varepsilon)C_{vg} + \varepsilon C_l L}{1-\varepsilon+\varepsilon K^2}$$

We define

$$\bar{k} = \frac{\bar{C}_p}{\bar{C}_v} = k \cdot \frac{1+\frac{\varepsilon}{1-\varepsilon}\delta L}{1+k\cdot\frac{\varepsilon}{1-\varepsilon}\delta L} \tag{13}$$

Let

$$\bar{C}_p = \frac{\bar{k}}{\bar{k}-1} A_0 \bar{R}$$

$\bar{k}$ and $\bar{R}$ are, respectively, the constant lag specific heat ratio and gas constant of the combustion chamber. When $K = L = 0$, $\bar{k} = k$, $\bar{R} = R_g$, and we have pure gas phase flow. When $K = L = 1$,

$$\bar{k} = k \cdot \frac{1+\frac{\varepsilon}{1-\varepsilon}\delta}{1+k\frac{\varepsilon}{1-\varepsilon}\delta}, \quad \bar{R} = (1-\varepsilon)R_g,$$

corresponding to two-phase equilibrium flow. Fig. 1 shows the variation of $\bar{k}$ and $\bar{R}$ with particle velocity lag (1-K).

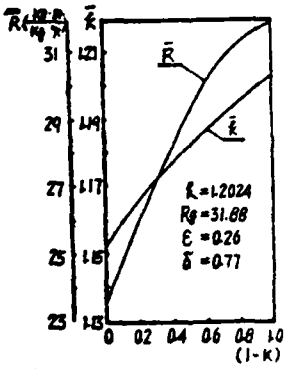

Fig. 1. Effect of particle velocity lag on $\bar{k}$ and $\bar{R}$

After introducing $\bar{k}$ and $\bar{R}$, we obtain from Eq. (11)

$$\frac{T_g}{T_0} = 1 - \frac{\bar{k}-1}{\bar{k}+1}\lambda^2 = \tau(\lambda) \tag{15}$$

In the above equation,

$$\lambda = \frac{v_g}{a_{cr}} \tag{16}$$

$$a_{cr} = \sqrt{\frac{2}{k+1} k g R T_0} \tag{17}$$

$\bar{\lambda}$ is termed the velocity coefficient of the constant lag flow. It is also a notation adopted for the purpose of obtaining a solution similar in form to that for pure gas phase, and does not represent the actual velocity coefficient of the gas phase. $\bar{a}_{cr}$ is termed the constant lag critical sound velocity. It varies with K because $\bar{k}$ and $\bar{R}$ have different values for different values of K.

2. Pressure Ratio $\frac{P}{P_0}$

Substituting $v_p = K v_g$, and $\frac{\rho_g v_p}{\rho_g v_g} = \frac{e}{1-e}$ into Eq. (5), we obtain

$$\frac{P}{P_0} = \frac{1 - \frac{\bar{k}-1}{\bar{k}+1}\bar{\lambda}^2}{1 + a\bar{\lambda}^2} = r(\bar{\lambda}) \tag{18}$$

In the above equation /5

$$a = \frac{2\bar{k}\varphi - \bar{k} + 1}{\bar{k}+1} \tag{19}$$

$$\varphi = \frac{1 + \frac{e}{1-e}K}{1 + \frac{e}{1-e}K^2} \tag{20}$$

3. Density Ratio $\frac{\rho_g}{\rho_0}$

From the state equation of the ideal gas,

$$\frac{\rho_g}{\rho_0} = \frac{P}{P_0} \cdot \frac{T_0}{T_g}$$

Substituting Eqs. (15) and (18) into the above equation, we get

$$\frac{\rho_g}{\rho_*}=\frac{1}{1+a\lambda^2} \tag{21}$$

ρ_* is the gas phase density at the grain head.

4. Total Pressure Ratio $\frac{P_s}{P_*}$

The ratio of the gas phase stagnation pressure P_S at any cross-section of the grain passage to the pressure P_O at the grain head is

$$\frac{P_s}{P_*}=\frac{P_s}{P}\cdot\frac{P}{P_*} \tag{a}$$

On the other hand,

$$\frac{P_s}{P}=\left(\frac{T_s}{T_g}\right)^{\frac{k}{k-1}} \tag{b}$$

T_S is the gas phase stagnation temperature at that particular cross-section.

The gas phase parameters at the same cross-section satisfy the equation

$$C_{pg}T_g+A_Q\frac{v_1^2}{2g}=C_{pg}T_s$$

It follows that

$$\frac{T_s}{T_g}=\frac{A_Q}{2g}\cdot\frac{v_1^2}{C_{pg}\frac{T_g}{T_*}\cdot T_*}+1$$

Substituting Eqs. (15) and (16) into the above equation, we obtain, after some rearrangement,

$$\frac{T_s}{T_g}=1+\frac{C_p}{C_{pg}}\cdot\frac{\frac{k-1}{k+1}\lambda^2}{1-\frac{k-1}{k+1}\lambda^2} \tag{c}$$

Inserting Eqs. (18), (b) and (c) into Eq. (a), we have

$$\frac{p_s}{P_0}=\frac{\left[1+\left(\frac{\bar{C}_p}{C_{p_g}}-1\right)\frac{k-1}{k+1}\lambda^2\right]^{\frac{k}{k-1}}}{(1+a\lambda^2)\left(1-\frac{k-1}{k+1}\lambda^2\right)^{\frac{1}{k-1}}}=\sigma(\lambda) \tag{22}$$

5. Total Temperature Ratio $\frac{T_s}{T_0}$ /6

$$\frac{T_s}{T_0}=\frac{T_s}{T_g}\cdot\frac{T_g}{T_0}$$

Substituting Eqs. (15) and (c) into the above, we obtain

$$\frac{T_s}{T_0}=1+\left(\frac{\bar{C}_p}{C_{p_g}}-1\right)\cdot\frac{k-1}{k+1}\lambda^2 \tag{23}$$

Therefore, the total temperature of the gas phase varies along the length of the passage. This is due to the fact that, in the flow, the particles transfer heat to the gas phase, the gas has to overcome friction due to the particles in order to do work, and the gas phase flow process is not an adiabatic process.

6. Parameters of the Particles

The flow parameters of the particles are calculated from the following equations:

$$\left.\begin{aligned} v_p&=Kv_g\\ T_p&=(1-L)T_0+LT_g\\ \rho_p&=\frac{\varepsilon}{(1-\varepsilon)K}\rho_g \end{aligned}\right\} \tag{24}$$

IV. Relation between J and $\bar{\lambda}_L$

From conversation of mass,

$$\left.\begin{aligned} \dot{m}_L&=\dot{m}_1\\ \dot{m}_L&=A_p(\rho_{gL}v_{gL}+\rho_{pL}v_{pL})\\ &=A_p\rho_{gL}v_{gL}\left(1+\frac{\varepsilon}{1-\varepsilon}\right) \end{aligned}\right. \tag{d}$$

$$= \frac{1}{1-\varepsilon} A_p \frac{\rho_{gL}}{\rho_0} \rho_0 \cdot \bar{\lambda}_L \bar{a}_{gr} \qquad \text{(e)}$$

From one-dimensional steady constant two-phase constant lag nozzle flow theory[2], [3]

$$\dot{m}_t = \frac{1}{1-\varepsilon} \frac{\bar{\Gamma}}{\sqrt{gR_g T_0 C}} P_{sL} A_t \sqrt{\frac{k}{\tau}} \qquad \text{(f)}$$

In the above equation

$$\tau = 1 + (k-1)\frac{\bar{D}}{C}$$

$$D = \frac{1 + \frac{\varepsilon}{1-\varepsilon} K^2}{1 + \frac{\varepsilon}{1-\varepsilon} \delta L}$$

$$C = 1 + \frac{\varepsilon}{1-\varepsilon} \{K[k(1-K)+K] + (k-1)\delta L D\}$$

$$\Gamma = \sqrt{\tau} \left(\frac{2}{\tau+1}\right)^{\frac{\tau+1}{2(\tau-1)}}$$

Substituting Eqs. (e), (f) into Eq. (d), and noting /7
that $P_{sL} = P_0 \sigma(\bar{\lambda}_L)$, $P_0 = \rho_0 g R_g T_0$, we obtain

$$J = \frac{A_t}{A_p} = \frac{\left(1 - \frac{k-1}{k+1}\bar{\lambda}_L^2\right)^{\frac{1}{k-1}} \cdot \bar{\lambda}_L \cdot \xi}{\left[1 + \left(\frac{C_p}{C_{p0}} - 1\right)\frac{k-1}{k+1}\bar{\lambda}_L^2\right]^{\frac{k}{k-1}}} \qquad (25)$$

In the above equation,

$$\xi = \frac{1}{\Gamma}\sqrt{\frac{2}{k+1}\frac{k}{k}\frac{\bar{R}}{R_g}\tau C}$$

It can thus be seen that, with respect to constant lag flows, there exists a definite relation between the $\bar{\lambda}_L$ at the tail end of the grain and the throat-passage ratio J. When all

the other parameters are fixed, $\bar{\lambda}_L$ is solely determined by J.

V. Equilibrium Pressure P_0 at Grain Head

To emphasize the study of the effects of the two-phase flow in the combustion chamber on the performance of the inner trajectory, we will discuss only the case for smaller values of J (eg. $J < 0.4$). In this case, the flow velocity is relatively low, and the effect of flow is not serious, so that one may regard the combustion rate r to be constant along the entire length of the passage, and equal to that at the grain head; i.e., $r = r_0 = bP_0^{n}$[4]. It follows that the rate of increase of mass of the products of combustion is

$$\dot{m}_b = \rho_T \cdot b P_0^n \cdot A_b \tag{g}$$

From the assumption of instantaneous equilibrium, $\dot{m}_b = \dot{m}_t$.

Inserting Eqs. (f) and (g) into the above equation, we obtain after some rearrangement

$$P_0 = \left[C^* \rho_T b K_1 \frac{1}{\sigma(\bar{\lambda}_L) \cdot \psi} \right]^{\frac{1}{1-n}} \tag{26}$$

In the above equation,

$$\psi = \frac{1}{1-\epsilon} \frac{\bar{\Gamma}}{\Gamma} \sqrt{\frac{k}{r} \frac{1}{C}}$$

$$K_1 = \frac{A_b}{A_t}$$

$$\Gamma = \sqrt{k} \left(\frac{2}{k+1} \right)^{\frac{k+1}{2(k-1)}}$$

VI. Distribution of $\bar{\lambda}$ along X

Integrating Eq. (1) from 0 to x, we obtain

As

$$\dot{m} = \rho_T r_0 S x$$

$$\dot{m} = A_p(\rho_g v_g + \rho_p v_p) = \frac{1}{1-\varepsilon} A_p \rho_g v_g$$

we have

$$\frac{1}{1-\varepsilon} A_p \rho_g v_g = \rho_T r_0 S x$$

Similarly,

$$\frac{1}{1-\varepsilon} A_p \rho_{gL} v_{gL} = \rho_T r_0 S l$$

Dividing the last equation into the one before, we have /8

$$\frac{\rho_g v_g}{\rho_{gL} v_{gL}} = \frac{x}{l} = \bar{x}$$

i.e.

$$\frac{\frac{\rho_g}{\rho_0} \cdot \bar{\lambda}}{\frac{\rho_{gL}}{\rho_0} \cdot \bar{\lambda}_L} = \bar{x}$$

Inserting Eq. (21) into the above equation, we obtain after some rearranging,

$$\bar{\lambda} = \left[\frac{1 + a\bar{\lambda}_L^2}{\bar{\lambda}_L} - \sqrt{\left(\frac{1 + a\bar{\lambda}_L^2}{\bar{\lambda}_L} \right)^2 - 4a\bar{x}^2} \right] \Big/ 2a\bar{x} \qquad (27)$$

It can be seen from Eqs. (15), (18), (21), (22), (25), (26) and (27) that the various relations pertaining to the constant lag two-phase flow in the combustion chamber are similar to the corresponding relationships pertaining to the pure gas phase. When K = L = 0, we obtain the relations for the pure gas flow; when K = L = 1, we obtain the relations for the two-phase equilibrium flow. Therefore, the pure gas phase flow and the two-phase equilibrium flow can be regarded as special cases on the constant lag flow.

VII. Relationship between the Lag Constants K and L

From the mass equation, momentum and energy equation of the particles given in Ref. [1], we can derive

$$\frac{dv_p}{dx} = \frac{A(v_g - v_p)}{v_p} - W_p \frac{S}{A_p} \tag{28}$$

$$\frac{dT_p}{dx} = \frac{1}{v_p C_{lg}} \left[\frac{A_0}{2} W_p \frac{S}{A_p} (W_p^2 + v_p^2) - B(T_p - T_g) \right] \tag{29}$$

Under the conditions of the combustion chamber, the particles maintain their Stokes flow state[2], and

$$\left.\begin{aligned} A &= \frac{9}{2} \frac{\mu_g}{r_p^2 \rho_{mp}} \\ B &= \frac{3\lambda_g}{r_p^2 \rho_{mp}} \end{aligned}\right\} \tag{30}$$

From the definition of constant lag flow,

$$dv_p = K dv_g$$

$$dT_p = L dT_g$$

Substituting the above into Eqs. (28) and (29), respectively, we obtain

$$\left.\begin{aligned} \frac{dv_g}{dx} &= \frac{A(1-K)}{K^2} - \frac{W_p}{K} \frac{S}{A_p} \\ \frac{dT_g}{dx} &= \frac{1}{KLv_g C_{lg}} \left[\frac{A_0}{2} W_p \frac{S}{A_p} (W_p^2 + K^2 v_g^2) - B(1-L)(T_g - T_g) \right] \end{aligned}\right\} \tag{h}$$

From Eq. (11), we have

$$\left.\begin{aligned} \frac{dT_g}{dx} &= -\frac{A_0}{g\bar{C}_p} v_g \frac{dv_g}{dx} \\ T_s - T_g &= A_0 \frac{v_g^2}{2g\bar{C}_p} \end{aligned}\right\} \tag{i}$$

Inserting Eq. (i) into Eq. (h), we get /9

$$\frac{dv_g}{dx}=-\frac{\bar{C}_p}{KLC_l}\left[\frac{1}{2}W_p\frac{S}{A_p}\left(\frac{W_p^2}{v_g^2}+K^2\right)-B(1-L)\frac{1}{2g\bar{C}_p}\right]$$

Comparing the two expressions for $\frac{dv_g}{dx}$, we obtain

$$L=\frac{\frac{B}{2gC_l}K-\frac{1}{2}\frac{\bar{C}_p}{C_l}W_p\frac{S}{A_p}\left(\frac{W_p^2}{v_g^2}+K^2\right)K}{A-\left(A+W_p\frac{S}{A_p}-\frac{B}{2gC_l}\right)K} \tag{31}$$

In the combustion chamber of the solid propellant rocket engine, A and $\frac{B}{2gC_l}$ are on the order of magnitude of 10^5 (1/sec),

$$W_p\frac{S}{A_p}\ll A$$

$$\frac{\bar{C}_p}{C_l}W_p\frac{S}{A_p}\left(\frac{W_p^2}{v_g^2}+K^2\right)\ll\frac{B}{gC_l}$$

Therefore, Eq. (31) can be simplified as

As $$L=\frac{1}{\frac{1-K}{K}2gC_l\frac{A}{B}+1}$$

$$\frac{A}{B}=\frac{3}{2}P_r\frac{1}{gC_{Pg}}$$

we have $$L=\frac{1}{3P_r\frac{C_l}{C_{Pg}}\frac{1-K}{K}+1} \tag{32}$$

This relationship is similar to that between the lag constants for the one-dimensional two-phase constant lag flow in the nozzle. Thus, the chief factor affecting the relationship between the lag constants is still the interaction of heat and forces between the particles and the gas phase. The effect f the particle jet velocity W_p can be neglected. Eq. (32) shows that when C_l and C_{Pg} are constant, if K has a definite value, then the

value of L is also definite. In many engineering applications, 5 [2], and $0 \leq K \leq 1$. Hence $L \leq K$, or $1 - L \geq 1 - K$. This shows that in constant lag flows, the temperature lag of the particles is greater than their velocity lag. The relationship between L and K is as shown in Fig. 2.

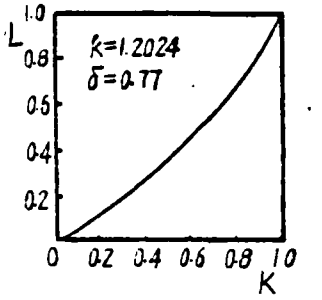

Fig. 2. Relationship between the lag constants K and L

VIII. Effect of Particle Velocity Lag on Inner Trajectory Performance

In reference to a particular solid propellant rocket engine ($\varepsilon = 0.26$), we have calculated the P-t curves and the flow fields of the combustion chamber for different values of K.

Fig. 3 shows the pressure-time curves for different values of K. It can be seen from this diagram that the pressure in the combustion chamber with velocity lag is lower than that of the two-phase equilibrium flow. Furthermore, the larger the particle velocity lag, the lower the pressure. The reduction in pressure of the combustion chamber results in a reduced combustion rate, causing the burning time of the grain to increase, and the amount of flow to decrease. Table 1 gives a list of the variation with particle velocity lag, at $t = 0$, of the constant lag flow combustion chamber pressure, grain burning time and the ratio of the mass flow per second to that corresponding to the two-phase equilibrium flow.

Fig. 4 shows the distribution along the length of the /10 passage of the constant lag velocity coefficient $\bar{\lambda}$ and the

Table 1

$1-K$	0	0.1	0.2	0.3	0.4	0.5	0.6	0.7	0.8	0.9
$P_s/P_{s,e}$	1.000	0.983	0.966	0.949	0.931	0.914	0.895	0.876	0.856	0.836
$t_s/t_{s,e}$	1.000	1.003	1.007	1.010	1.014	1.018	1.021	1.025	1.030	1.035
$\dot{m}_s/\dot{m}_{s,e}$	1.000	0.997	0.994	0.990	0.987	0.983	0.979	0.975	0.971	0.967

relative gas phase parameters. It can be seen from the diagram that $\frac{P}{P_e}$, $\frac{P_s}{P_e}$, $\frac{T_g}{T_e}$ and $\frac{\rho_g}{\rho_e}$ all decrease along the passage length, while λ increases along the length. The trends of variations are similar to those for the two-phase equilibrium flow. The values are slightly lower than the corresponding values for the two-phase equilibrium flow, but the differences are very small. This illustrates that the particle velocity lag has but minor effects on the distribution of the relative values of the gas phase parameters along the passage length. As P_O decreases with the increase of particle velocity lag, the distribution of P, P_S and ρ_g along the passage length is more severely affected by the velocity lag. It can be seen from fig. 5 that the values of these parameters are all smaller than those for the two-phase equilibrium flow, and the greater the velocity lag, the lower these values. However, the particle velocity lag has very little effect on the distribution of T_g.

The distribution of the gas phase velocity v_g and the particle velocity v_p along the passage length under different lag conditions at t = 0 is shown in Fig. 6. All the values increase along the passage length, characteristic of the introduction of mass. However, K has opposite effects on v_g and v_p. It can be seen from the diagram that in the presence of a lag, v_p has a lower value than that of the two-phase equilibrium flow: the greater the lag, the smaller v_p. On the other hand, v_g has a higher value than that for the two-phase equilibrium flow; the greater the lag, the greater v_g. This is because when (1 - K)

increases, both $\bar{k}$ and $\bar{R}$ increase, causing $\bar{a}_{cr}$ to increase, while the particle velocity lag has a very small effect on $\bar{\lambda}$. Therefore, when (1 - K) increases, v_g increases. From the standpoint of physical significance, the value of K actually reflects the size of the particles. A large velocity lag (small K) signifies a large size of the particles. We know from Eq. (30) that $A \propto \frac{1}{r_p^2}$. Hence. for a large lag, A is small, the drag $X = A(v_g - v_p)$ exerted on the gas phase by a unit mass of particle is small, and as a result, the gas phase velocity is large. Of course, under such conditions, the force with which the gas phase carries the particles along is also small. The particles have a low acceleration, and their velocity is low.

The distribution of the temperature and density of the particles along the length of the passage is shown in Fig. 7. The decrease of ρ_p, and T_p along the passage is very small. The particle velocity lag has an extremely small effect on the distribution of T_p, but a rather large effect on the distribution of ρ_p. It can be seen from the diagram that the value of ρ_p in the presence of lag is higher than that for the two-phase equilibrium flow, and the greater the lag, the greater the value of ρ_p.

The results of computations show that the total temperature T_s of the gas phase changes very slightly along the passage. For instance, for 1 - K = 0.9 and t = 0, t_0 = 3042.4°K at the head, while T_{SL} = 3042.46°K at the end of the grain passage. The increase is only 0.06°K. Actually, as $\frac{\bar{C}_p}{C_{ps}}$ in Eq. (23) is very close to unity, T_s can be considered as being constant along the passage in the computation. As a result, Eqs. (22) and (25) can be simplified to

$$\frac{P_s}{P_0} = \left[(1+a\bar{\lambda}^2)\left(1-\frac{k-1}{k+1}\bar{\lambda}^2\right)^{\frac{1}{k-1}}\right]^{-1} \tag{22'}$$

$$J = \left(1-\frac{k-1}{k+1}\bar{\lambda}_L^2\right)^{\frac{1}{k-1}} \cdot \bar{\lambda}_L \cdot \xi \tag{25'}$$

IX. Conclusion /11

We can conclude from the above discussion that:

1. The fundamental relations for the one-dimensional two-phase constant lag flow in solid propellant rocket engines are similar to those for the pure gas phase flow. Pure gas phase flow and two-phase equilibrium flow can both be regarded as special cases of constant lag flow. Therefore, the method presented in this paper for inner trajectory computations has greater generality.

2. Owing to the effect of the particle velocity lag, the pressure in the combustion chamber decreases, the burning time of the grain is lengthened, and the nozzle flow is reduced.

3. Two-phase flow has a relatively large effect on the flow field of the combustion chamber. With increasing particle velocity lag, the gas phase flow rate increases, pressure, total pressure and gas phase density decrease, particle velocity decreases, and particle density increases. However, the particle velocity lag has little effect on the temperature of the gas phase and the particles.

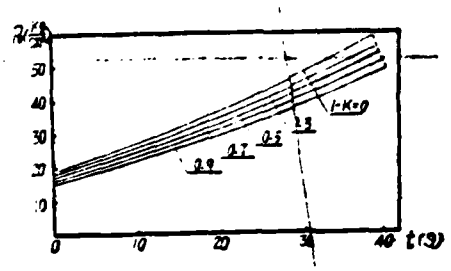

Fig. 3. Pressure-time curves

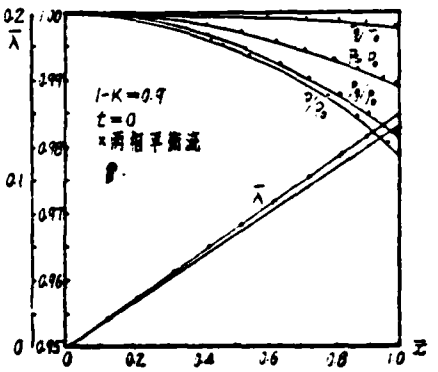

Fig. 4. Distribution of relative values of gas phase parameters in two-phase flow

Key: 1) two-phase equilibrium flow

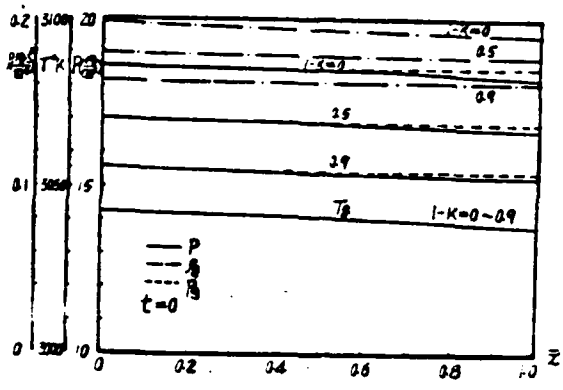

Fig. 5. Distribution of gas phase parameters in two-phase flow

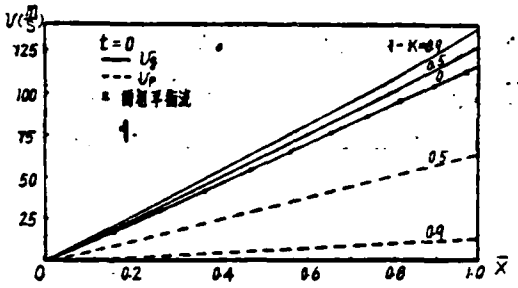

Fig. 6. Distribution of velocity of the gas and the particles in two-phase flow

Key: 1) two-phase equilibrium flow

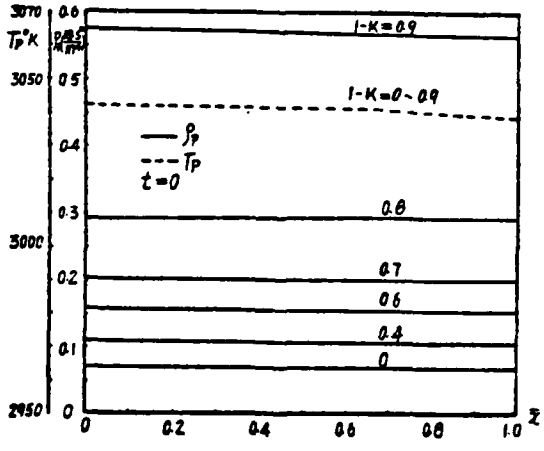

Fig. 7. Distribution of particle parameters in two-phase flow

REFERENCES

[1] AD 766 567, Chapter VI, 1973.

[2] Joe D. Hoffman, Gas Dynamics, Volume II, P53-66, 1977.

[3] Fang Tin-yu, Two-Phase Flows in Solid Propellant Rocket Engines, National Defense Technological College, 1982

[4] Design Fundamentals of Solid Propellant Rocket Engines, Volume 1, Ch'angsha School of Engineering, 1976.


ATE
LME